

Achieving fair sampling in quantum annealing

Vaibhaw Kumar¹, Casey Tomlin¹, Curt Nehr Korn¹, Daniel O'Malley², Joseph Dulny III¹

¹*Booz Allen Hamilton*

²*Los Alamos National Laboratory*

(Dated: September 9, 2020)

Sampling all ground states of a Hamiltonian with equal probability is a desired feature of a sampling algorithm, but recent studies indicate that common variants of transverse field quantum annealing sample the ground state subspace unfairly. In this note, we present perturbation theory arguments suggesting that this deficiency can be corrected by employing reverse annealing-inspired paths. We confirm that this conclusion holds in simulations of previously studied small instances with degeneracy, as well as larger instances on quantum annealing hardware.

Quantum annealing (QA)-based optimization has gained a lot of interest recently, fueled partially by the advent of QA hardware [1]. The usual aim of this technique is to produce a ground state of a Hamiltonian cost function with sufficiently high probability, with less attention paid to the distribution of sampled solutions. In cases where there are several cost function minima, one would hope to find that each is sampled with equal probability across many annealing runs; i.e., one would like a protocol that achieves *fair sampling*. Fair sampling is crucial for a number of applications. One such example, the *set membership problem*, ubiquitous in computer science [2–4], involves finding whether an element belongs to a given set. SAT-based probabilistic membership filters [5–9] used to establish set membership require access to not one, but a majority of the solutions of the underlying SAT problem. Other applications for which fair sampling is important include ground state entropy calculations, counting problems [10, 11], and machine learning [12, 13].

“Vanilla” quantum annealing involves evolution with respect to a Hamiltonian

$$H(t) = (1 - t/T)H_d + (t/T)H_p, \quad t \in [0, T], \quad (1)$$

where T is the total evolution time, H_p is the ‘problem’ Hamiltonian, diagonal in the z -basis, whose ground states are sought, and H_d is a ‘driver’ Hamiltonian capable of inducing transitions between z -eigenstates (usually $-\sum \sigma_i^x$). For sufficiently large T , the adiabatic theorem [14] promises that the instantaneous ground state of $H(t)$ is approximately tracked throughout the evolution, so that a z -basis measurement at $t = T$ should return a ground state of H_p .

Perturbation theory arguments, simulations of small toy models, and actual QA hardware experiments on relatively large 2D square lattice spin models indicate that this simple protocol fails to sample degenerate ground states fairly [15–21]. In such cases, some of the ground states are “hard” suppressed (the probability of observing these states is approximately zero). Other cases feature “soft” suppression: all ground states are observed with non-zero probability, but some are seen more frequently than others. Soft suppression is usually repairable with a sufficient number of annealing runs

and post-processing, but hard suppression is particularly detrimental for certain applications, such as those mentioned above.

In principle, a denser transverse driver can mitigate the sampling bias, but such drivers are difficult both to engineer, and to simulate classically [15, 18]. As observed in [18], even dense drivers cannot completely remove sampling bias, except in the extreme case of a complete graph driver. Another recent proposal [22] based on “extended” quantum annealing [23] also appears to be difficult to realize experimentally.

In this note, we use perturbation theory arguments similar to those used in [18] to suggest a simple solution to the fair sampling problem, based on reverse annealing [24]. In particular, we consider random diagonal perturbations of the final Hamiltonian, which in perturbation theory trivially break degeneracy, leading to a uniform choice of computational basis state from the originally degenerate subspace in each run. We verify that these perturbation theory arguments are borne out via simulations of the small systems described in [18]. Though we do not take into account time-dependent effects in the perturbative arguments, we believe that their inclusion should only serve to mitigate the problem further (via late-time transitions to excited states).

Perturbation theory: Let $s := t/T$ be a dimensionless time parameter. Towards the end of the anneal, where $1 - s \ll 1$ (or rather when $s \approx 1 - \lambda$ with $\lambda \ll 1$), $H(1 - \lambda)$ can be viewed as a perturbation of the problem Hamiltonian H_p by the driver H_d ¹.

$$H(1 - \lambda) = H_p + \lambda H_d + O(\lambda^2) \quad (2)$$

If H_p has m degenerate (computational basis) ground states $|g_i\rangle, i \in \{1, \dots, m\}$ with energy $E^{(0)}$, switching on the perturbation will result in the splitting of those states into m eigenstates of $H(1 - \lambda)$ with distinct energies². Perturbation theory posits that the energies $E_k(\lambda)$

¹ At this stage we are assuming exact adiabatic evolution and ignoring time-dependent effects.

² If the degeneracy is not completely lifted by the perturbation at first order, some of these eigenstates will share the same energy, but in the protocol described below this is rare.

and eigenstates $|k\rangle_\lambda, k \in \{1, \dots, m\}$ of $H(1 - \lambda)$ can be expressed as a power series in λ :

$$E_k(\lambda) = E^{(0)} + \lambda E_k^{(1)} + O(\lambda^2) \quad (3)$$

$$|k\rangle_\lambda = |k^{(0)}\rangle + \lambda |k^{(1)}\rangle + O(\lambda^2) \quad (4)$$

Inserting these Ansätze into the (time-independent) Schrödinger equation, one can compute corrections to the states and energies order by order in λ in terms of quantities known from the unperturbed system [25]. For the resulting analysis to remain consistent, one must identify a “good” basis for the degenerate ground state subspace that diagonalizes a given perturbation. More specifically, suitable β_k^i that define good basis states $|k^{(0)}\rangle = \sum_{i=1}^m \beta_k^i |g_i\rangle$ must be determined. β_k^i can be obtained by solving the eigenvalue problem $W\beta_k = \epsilon_k \beta_k$ with $W_{ij} := \langle g_i | V | g_j \rangle$. Here, eigenvalues ϵ_k provide the first order energy corrections $E_k^{(1)}$, the smallest of which enters the instantaneous ground state energy $E_{\tilde{k}} = E^{(0)} + \lambda E_{\tilde{k}}^{(1)}$ of $H(1 - \lambda)$ (where we have designated $\tilde{k} := \operatorname{argmin}_k \epsilon_k$).

As pointed out in [18], perturbation theory provides a simple explanation as to why some ground states are hard-suppressed in QA: Assuming exact adiabaticity, the corresponding eigenstate $|\tilde{k}\rangle = \sum \beta_{\tilde{k}}^i |g_i\rangle$ dictates the sampling probabilities in the computational basis; in particular, $\beta_{\tilde{k}}^i = 0$ leads to hard suppression of the i^{th} degenerate ground state of H_p since the state being tracked by adiabatic evolution has no support on $|g_i\rangle$ near the end of the anneal. This suppression is caused by the sparse nature of the standard hypercube driver $V = -\sum \sigma^x$ as perturbation, and the set of ground states of H_p . Occasionally one can get lucky when using V , with all ground states reachable from each other by single bit flips, in which case soft suppression is a worst-case scenario. But this is not the case in general, even with denser drivers—only for the complete graph driver are we guaranteed that the late-time instantaneous ground state has support on all ground states of H_p . Unfortunately, engineering anything close to the complete graph driver seems prohibitively difficult. This compels us to search for alternative drivers that provide support for a would-be suppressed $|g_i\rangle$, at least in a perturbative analysis, if we seek to cure this suppression.

$$\begin{pmatrix} \mu(\gamma_0) & 0 & 0 & 0 & 0 & 0 & 0 & 0 \\ 0 & \mu(g_0) & 0 & 0 & 0 & 0 & 0 & 0 \\ 0 & 0 & \mu(\gamma_1) & 0 & 0 & 0 & 0 & 0 \\ 0 & 0 & 0 & \mu(g_1) & 0 & 0 & 0 & 0 \\ 0 & 0 & 0 & 0 & \mu(\gamma_2) & 0 & 0 & 0 \\ 0 & 0 & 0 & 0 & 0 & \mu(\gamma_3) & 0 & 0 \\ 0 & 0 & 0 & 0 & 0 & 0 & \mu(g_2) & 0 \\ 0 & 0 & 0 & 0 & 0 & 0 & 0 & \mu(\gamma_4) \end{pmatrix} \quad \beta_{\tilde{k}} \text{ is either } \begin{pmatrix} 1 \\ 0 \\ 0 \end{pmatrix} \text{ or } \begin{pmatrix} 0 \\ 1 \\ 0 \end{pmatrix} \text{ or } \begin{pmatrix} 0 \\ 0 \\ 1 \end{pmatrix}$$

FIG. 1. Schematic showing H_z for the $m = 3$ case. Highlighted rows indicate the subspace spanned by the ground states $\{|g_1\rangle, |g_2\rangle, |g_3\rangle\}$. The reduced matrix (bottom left) in the ground state subspace has eigenvalues which supports either of the ground states.

Diagonal perturbations: We argue here that adding diagonal Hamiltonians of the ‘reverse annealing’ type to the driver can mitigate biased sampling. In particular, we consider

$$H_z = \sum_i c_i \sigma_i^z \quad (5)$$

with c_i drawn randomly from a normal distribution. Since H_z is diagonal, its eigenstates are computational basis states, and if H_z were the only term to $O(\lambda)$ in the perturbed Hamiltonian, then the good basis that diagonalizes H_z in the ground state subspace of H_p is simply composed of the degenerate computational basis ground states $|g_i\rangle$ themselves. It follows that the $|g_i\rangle$ with the smallest H_z eigenvalue will be favored in measurements. As we describe further below, running multiple anneals, each with a different perturbation characterized by randomly chosen c_i , will encourage each ground state of H_p to be measured with roughly equal probability.

Properties of H_z : For c_i picked randomly from a normal distribution with zero mean and unit variance, in the ground state subspace spanned by some of the $|g_j\rangle$ (see Fig 1), the corresponding eigenvalues are

$$\mu(g_j) = \sum_{i=1}^n (-1)^{g_j(i)} c_i \quad (6)$$

where $g_j(i)$ represents the bit value of $|g_j\rangle$ at the i^{th} position. Since each eigenvalue is a linear combination of the c_i , they are also normally distributed, and across many instantiations, $\operatorname{argmin}_j \mu(g_j)$ is distributed uniformly; that is, a preferred degenerate computational basis state will be chosen uniformly at random in each annealing run to dominate the support of instantaneous ground state near the end of the anneal. In order to observe all m degenerate ground states, an expected

$\Theta(m \log m)$ runs are required.³

Reverse annealing: Feasibly engineerable time-dependent Hamiltonians that feature terms like H_z as perturbations of H_p at late times are present in so-called reverse annealing schemes [26–28], which fall under a broader class of protocols that employ non-convex combinations of initial and final Hamiltonians. Here we consider Hamiltonians of the type

$$H(s) = D(s)H_d + sH_p + Z(s)H_z, \quad (7)$$

where again $H_d = -\sum_i \sigma_i^x$ is the standard hypercube driver, H_p is the problem Hamiltonian, and $D(s)$ and $Z(s)$ are schedules which we specify further below. For our perturbation theory arguments, it is only necessary that

$$D(1 - \lambda) \approx O(\lambda^3), \quad (8)$$

$$Z(1 - \lambda) \approx O(\lambda). \quad (9)$$

The reverse annealing paradigm would further specify

$$D(\lambda) \approx O(\lambda), \quad (10)$$

$$Z(\lambda) \approx 1 - O(\lambda), \quad (11)$$

initializing the system in the ground state of H_z . The ground state $|\gamma_{\min}\rangle$ of H_z has eigenvalue $\mu(\gamma_{\min}) = \sum_{i=0}^{n-1} (-1)^{\gamma_{\min}(i)} c_i$ where $(-1)^{\gamma_{\min}(i)} c_i / |c_i| = -1$ for all i . These late-time conditions guarantee that the first-order perturbative corrections to the H_p eigenstates vanish⁴, but (except in very rare cases) the eigenvalues are split, resulting in a single H_p ground state providing the entire support of the instantaneous eigenstate.

Though perturbation theory is rather limited in what it can reliably say about the entire evolution (or the general utility of quantum annealing), its conclusions are corroborated by the simulated models considered here, which we describe below.

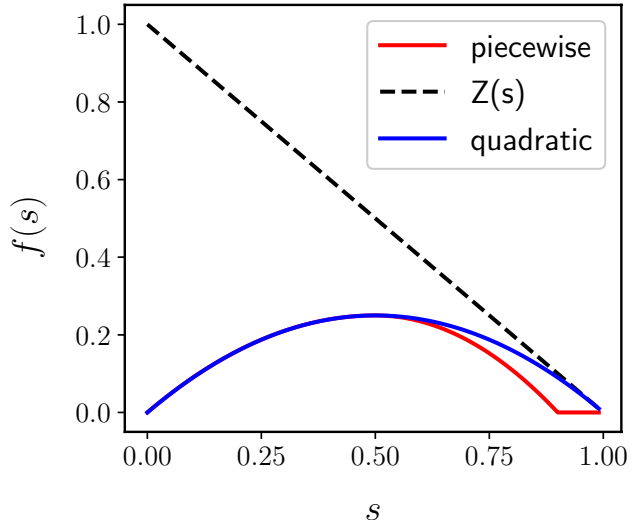


FIG. 2. Schedules considered. The red and blue lines indicate the transverse field piecewise and quadratic driver schedules, respectively. $Z(s)$ is shown in black.

For simulations, we fix the schedule $Z(s) = 1 - s$, and consider two schedules for the transverse field. These are shown in Figure 2; $D_q(s) = s(1 - s)$ is the quadratic driver schedule considered in [26], which violates (8) (and the looser condition in Footnote 4), but allows us to examine situations where a linear combination of H_d and H_z plays the role of the perturbation. Because the good basis is generally not a subset of the computational basis in this case, the perturbation theory arguments are not as trivial, but if the coefficient of H_z is sufficiently larger than that of H_d , then our conclusions should still hold approximately.

Contrast this with the piecewise schedule

$$D_{pw}(s) = \begin{cases} s(1 - s), & 0 \leq s < 0.5 \\ -\frac{25}{16}s^2 + \frac{25}{16}s - \frac{9}{64}, & 0.5 \leq s < 0.9 \\ 0, & 0.9 \leq s \leq 1.0 \end{cases}, \quad (12)$$

which ensures rather ham-handedly that the transverse field is absent in the perturbation. In this case we expect sampling probabilities to be solely dictated by H_z .

Small instances: Here we revisit the particular instances studied in [18] and shown in Figure 3. The problem

³ See the “coupon collector’s problem.” In the appendix we discuss the situation in which the number of ground states is not known in advance.

⁴ This can also be relaxed to $D(1 - \lambda) \approx O(\lambda^2)$ resulting in $O(\lambda)$ rotations of instantaneous eigenstates in the H_p ground state subspace, which does not affect our general arguments.

Hamiltonians are zero-bias Ising models

$$H_p = - \sum_{(i,j)} J_{ij} \sigma_i^z \sigma_j^z \quad (13)$$

and are depicted graphically in Figure 3, where each node corresponds to a qubit and each edge to a non-zero coupling J_{ij} . Consulting the figure, the coupling values are either 2 (dark red edges), 1 (orange edges), -1 (light blue edges), or -2 (dark blue edges). (a)-(c) have been shown to exhibit hard suppression while (d) features soft suppression.

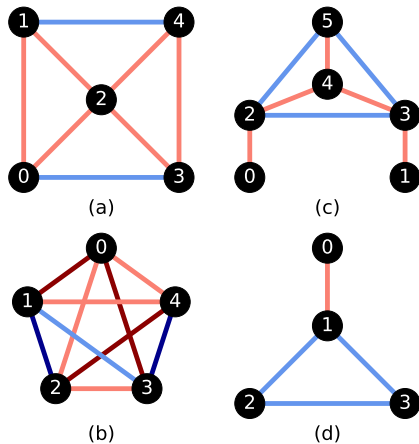


FIG. 3. The instances we consider. The coupling values are either 2 (dark red edges), 1 (orange edges), -1 (light blue edges), or -2 (dark blue edges).

Simulations: The perturbative arguments we have made so far only hold in the adiabatic limit. When time-dependence is taken into account and spectral gaps necessarily close, diabatic transitions will be induced. Though we do not provide an analytic argument, these transitions would presumably only further democratize sampling from the ground state subspace given the convergence of eigenvalues at late times. Indeed, the numerical simulations performed here appear to substantiate this intuition.

In Figure 4, we plot squared magnitude of each H_p ground state coefficient as a function of the total annealing time T , obtained by integrating the Schrödinger equation in Qutip [29, 30]. For the reverse annealing runs, we plot the average of these probabilities over multiple trials, where each trial corresponds to a randomly generated H_z , and we observe that this protocol does improve the sampling bias. In the case of the piecewise-defined schedule D_{pw} where H_z is the sole first-order perturbation to H_p at late times, we see that for all models, states that were suppressed by vanilla annealing now provide roughly equal support to the wave function for large enough T . We also observe that the quadratic driver schedule D_q , in which both H_d and H_z contribute at first order, is less effective at removing the bias in models (a) and (b).

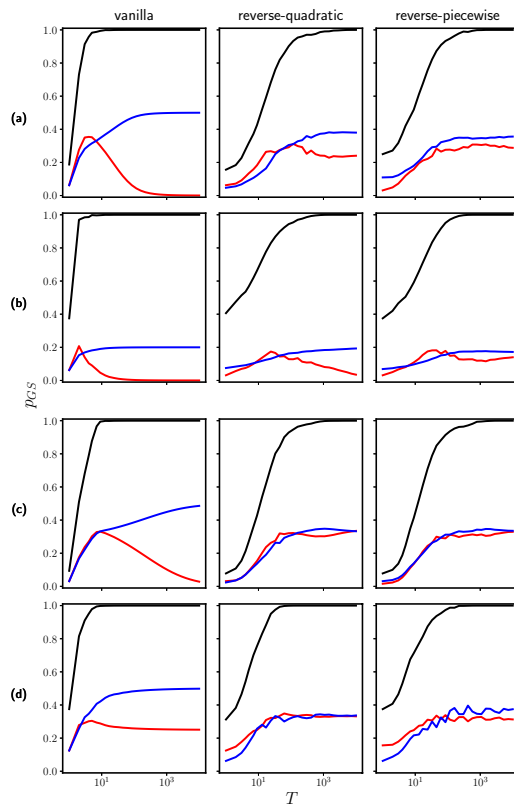


FIG. 4. Measurement probability versus total annealing time T for each of the ground states and schedules. Reverse annealing measurement probabilities were averaged over 32, 32, 64, and 16 trials for the models (a), (b), (c), and (d), respectively, where each trial corresponds to a randomly generated H_z . The labels correspond to the model labels in Figure 3. Red and blue curves show (up to symmetry) the probability of individual H_p ground states. The black curves show the sum of probabilities over all ground states.

Hardware runs: We have also examined larger spin glass instances supported on graphs native to D-Wave’s Chimera (using 160 qubits) and Pegasus (using 92 qubits) architectures. As in [21], we consider instances with couplings randomly drawn from $\{\pm 1, \pm 2, \pm 4\}$. For an initial pool of these instances, individual couplings are adjusted to keep the number of degenerate ground states manageable by eliminating so-called free spins (sites whose total local field vanishes; each of these doubles degeneracy)⁵. Then simulated annealing (SA) and parallel tempering with iso-energetic cluster moves (PT-ICM) (see Appendix A) were used to find the ground states of each instance, and those with the largest number of degenerate ground states were selected for additional classical analysis and quantum annealing runs. The latter were carried out on LANL’s D-Wave 2000Q system, and D-Wave’s Advantage system in Burnaby. To the best of our

⁵ This fairly expensive process was the main constraint on the size of the instances we considered.

knowledge, these machines do not allow a user to explicitly program the initial Hamiltonian (here H_z), but the same effect is achieved by programming an initial state (the would-be ground state of H_z), which is supported via reverse annealing functionality, and we simply specify uniformly chosen random initial states in these experiments. Outputs of the classical algorithms and quantum annealer runs were averaged over eight blocks of samples of size 500, obtained from independent trials, and we observed similar behavior in all of the instances and on both annealing devices. Results from an example instance based on a native Pegasus subgraph with 36-fold degeneracy are shown in Figure 5.

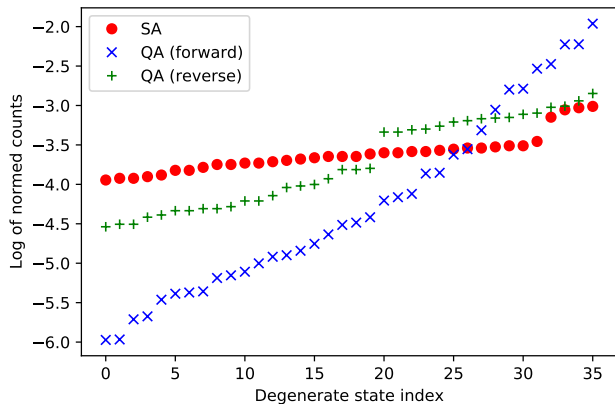


FIG. 5. Log of normed counts for each solution method. The horizontal axis simply enumerates the 36 ground states associated with this instance, and vertical axis corresponds to the (log of the) number of times that ground state was observed relative to the other ground states.

As expected, vanilla QA exhibits a substantial sampling bias (note that the vertical axis is log-scaled), while our

reverse annealing protocol performs comparably to simulated annealing. We point out however that, not surprisingly, the magnitude of the driver term (here controlled by an overall multiplicative factor of D_{pw}) plays an important role in the success or failure of our protocol; too large, and one is essentially back to vanilla annealing and the associate bias shows up; too small, and only a very small region near the initial state is explored (and indeed many ground states are never observed). In these experiments, we found that setting the driver term to $2D_{pw}H_d$ gave good results.

In the more realistic scenario where one does not know the dimension of the ground state subspace *a priori*, we give an algorithm in Appendix B that will return the full set of ground states (up to some specified failure tolerance), assuming the annealing protocol described here uniformly samples only the ground states. This latter assumption is of course dubious for contemporary devices, so additional multiplicative overhead is usually required.

Remarks: We have presented a very simple protocol, motivated by time-independent perturbation theory, that is able to cure a seemingly hard-wired tendency towards biased sampling afflicting vanilla quantum annealing. While it is well-known that the complete graph driver ensures fair sampling, no sparser driver can provide this guarantee in general, and in any case denser drivers seem extremely difficult to realize experimentally. On the other hand, since our method is very similar to existing reverse annealing techniques that have experimental realizations, it is also a practical solution to the unfair sampling problem.

I. ACKNOWLEDGEMENTS

We thank Michael Jarret for scathing comments on an initial draft and fruitful discussions, and D-Wave and Joel Gottlieb in particular for providing access to the Advantage system via their Beta program.

-
- [1] Zhengbing Bian, Fabian Chudak, William G Macready, and Geordie Rose. The ising model: teaching an old problem new tricks. *D-wave systems*, 2, 2010.
 - [2] Andrei Broder and Michael Mitzenmacher. Network applications of bloom filters: A survey. *Internet mathematics*, 1(4):485–509, 2004.
 - [3] Lukas Radvilavicius, L Marozas, and Antanas Cenys. Overview of real-time antivirus scanning engines. *Journal of Engineering Science & Technology Review*, 5(1), 2012.
 - [4] Sasu Tarkoma, Christian Esteve Rothenberg, and Eemil Lagerspetz. Theory and practice of bloom filters for distributed systems. *IEEE Communications Surveys & Tutorials*, 14(1):131–155, 2011.
 - [5] Sean A Weaver, Katrina J Ray, Victor W Marek, Andrew J Mayer, and Alden K Walker. Satisfiability-based set membership filters. *Journal on Satisfiability, Boolean Modeling and Computation*, 8(3-4):129–148, 2012.
 - [6] Thomas J. Schaefer. The complexity of satisfiability problems. In *Proceedings of the Tenth Annual ACM Symposium on Theory of Computing*, STOC 78, page 216226, New York, NY, USA, 1978. Association for Computing Machinery.
 - [7] Adam Douglass, Andrew D King, and Jack Raymond. Constructing sat filters with a quantum annealer. In *International Conference on Theory and Applications of Satisfiability Testing*, pages 104–120. Springer, 2015.
 - [8] Chao Fang, Zheng Zhu, and Helmut G Katzgraber. Nae-sat-based probabilistic membership filters. *arXiv preprint arXiv:1801.06232*, 2018.
 - [9] Marlon Azinović, Daniel Herr, Bettina Heim, Ethan Brown, and Matthias Troyer. Assessment of quantum

- annealing for the construction of satisfiability filters. *SciPost Physics*, 2(2):013, 2017.
- [10] Carla P Gomes, Ashish Sabharwal, and Bart Selman. Model counting: A new strategy for obtaining good bounds. In *AAAI*, pages 54–61, 2006.
- [11] Parikshit Gopalan, Adam Klivans, Raghu Meka, Daniel Štefankovic, Santosh Vempala, and Eric Vigoda. An fptas for # knapsack and related counting problems. In *2011 IEEE 52nd Annual Symposium on Foundations of Computer Science*, pages 817–826. IEEE, 2011.
- [12] Geoffrey E Hinton. Training products of experts by minimizing contrastive divergence. *Neural computation*, 14(8):1771–1800, 2002.
- [13] SM Ali Eslami, Nicolas Heess, Christopher KI Williams, and John Winn. The shape boltzmann machine: a strong model of object shape. *International Journal of Computer Vision*, 107(2):155–176, 2014.
- [14] Andris Ambainis and Oded Regev. An elementary proof of the quantum adiabatic theorem. *arXiv preprint quant-ph/0411152*, 2004.
- [15] Yoshiaki Matsuda, Hidetoshi Nishimori, and Helmut G Katzgraber. Ground-state statistics from annealing algorithms: quantum versus classical approaches. *New Journal of Physics*, 11(7):073021, 2009.
- [16] Tameem Albash, Walter Vinci, Anurag Mishra, Paul A Warburton, and Daniel A Lidar. Consistency tests of classical and quantum models for a quantum annealer. *Physical Review A*, 91(4):042314, 2015.
- [17] Sergio Boixo, Tameem Albash, Federico M Spedalieri, Nicholas Chancellor, and Daniel A Lidar. Experimental signature of programmable quantum annealing. *Nature communications*, 4:2067, 2013.
- [18] Mario S Könz, Guglielmo Mazzola, Andrew J Ochoa, Helmut G Katzgraber, and Matthias Troyer. Uncertain fate of fair sampling in quantum annealing. *Physical Review A*, 100(3):030303, 2019.
- [19] Andrew D King, Emile Hoskinson, Trevor Lanting, Evgeny Andriyash, and Mohammad H Amin. Degeneracy, degree, and heavy tails in quantum annealing. *Physical Review A*, 93(5):052320, 2016.
- [20] Brian Hu Zhang, Gene Wagenbreth, Victor Martin-Mayor, and Itay Hen. Advantages of unfair quantum ground-state sampling. *Scientific reports*, 7(1):1–12, 2017.
- [21] Salvatore Mandra, Zheng Zhu, and Helmut G Katzgraber. Exponentially biased ground-state sampling of quantum annealing machines with transverse-field driving hamiltonians. *Physical review letters*, 118(7):070502, 2017.
- [22] Masayuki Yamamoto, Masayuki Ohzeki, and Kazuyuki Tanaka. Fair sampling by simulated annealing on quantum annealer. *Journal of the Physical Society of Japan*, 89(2):025002, 2020.
- [23] Rolando D Somma, Cristian D Batista, and Gerardo Ortiz. Quantum approach to classical statistical mechanics. *Physical review letters*, 99(3):030603, 2007.
- [24] D-Wave. Reverse quantum annealing for local refinement of solutions, 9 2017.
- [25] Barton Zwiebach. Perturbation theory.
- [26] Alejandro Perdomo-Ortiz, Salvador E Venegas-Andraca, and Alán Aspuru-Guzik. A study of heuristic guesses for adiabatic quantum computation. *Quantum Information Processing*, 10(1):33–52, 2011.
- [27] Masaki Ohkuwa, Hidetoshi Nishimori, and Daniel A Lidar. Reverse annealing for the fully connected p-spin model. *Physical Review A*, 98(2):022314, 2018.
- [28] Yu Yamashiro, Masaki Ohkuwa, Hidetoshi Nishimori, and Daniel A Lidar. Dynamics of reverse annealing for the fully-connected p-spin model. *arXiv preprint arXiv:1906.10889*, 2019.
- [29] J Robert Johansson, Paul D Nation, and Franco Nori. Qutip 2: A python framework for the dynamics of open quantum systems. *Computer Physics Communications*, 184(4):1234–1240, 2013.
- [30] J Robert Johansson, PD Nation, and Franco Nori. Qutip: An open-source python framework for the dynamics of open quantum systems. *Computer Physics Communications*, 183(8):1760–1772, 2012.

Appendix A: Classical sampling schemes

Simulated annealing runs were carried out using D-Wave’s “neal” library functionality, and the PT-ICM Monte Carlo runs were performed using custom code. Two spin replicas at each β and 20 replicas were maintained at each β . A total of $N_{\text{sweep}} = 10^{14}$ MC sweeps were made, where each sweep consisted of: a) N single flips for a randomly selected spin replica at each β ; b) an iso-energetic clustering move between spin replicas at a randomly chosen β ; and c) parallel tempering swaps between a randomly chosen pair of β replicas. After $N_{\text{sweep}}/2$ sweeps, if both the spin replicas at the highest β were seen at the same energy, then that energy was recorded as the lowest energy. If a lower energy was observed after $> N_{\text{sweep}}/2$ sweeps, then the lowest energy was updated. Final samples at the highest β were obtained at the end of the run. For both SA and PT-ICM, a geometric β schedule was used, where the β range was set to $[\frac{1}{3.05}, \frac{1}{0.05}]$ with a bin size of 1.22.

Appendix B: An algorithm

We give an algorithm for generating (up to some failure rate) the set of all degenerate ground states G , assuming each is returned uniformly at random by the annealing procedure described in the main text. The key quantity is an estimate of the number of trials required to guarantee with high probability that all ground states have been observed. This is equivalent to the problem of determining the total number m of coupons in the coupon collector’s problem. For fixed m we have the following bound for the number of trials T required to collect all m coupons:

$$P[T > m \log(m/\epsilon)] \leq \epsilon \quad (\text{B1})$$

The algorithm below is composed of possibly several rounds of sampling, each round corresponding to an assumed m , and we use this inequality to bound the failure rate of the entire procedure. Specifically, if one asks for

a success rate of $1 - \epsilon$ after r rounds of sampling, one needs

$$T \geq \lceil m \log(rm/\epsilon) \rceil =: T(m, r, \epsilon) \quad (\text{B2})$$

samples per round. By iteratively doubling a guess for m as unseen states are sampled, we have that the maximum number of rounds is $n-1$ (for an n -qubit system; we begin with $m = 2$).

Algorithm1 GetGroundStates

Input: System size n , failure tolerance ϵ

Output: Set of ground states G

```

1:  $m \leftarrow 2$ 
2:  $T \leftarrow T(m, n, \epsilon)$ 
3:  $G \leftarrow \emptyset$ 
4:  $t \leftarrow 0$ 
5: while  $t \leq T$  do
6:    $g \leftarrow \text{ANNEALONCE}()$ 
7:    $G \leftarrow G \cup \{g\}$ 
8:    $t \leftarrow t + 1$ 
9:   if  $|G| > m$  then
10:     $m \leftarrow 2m$ 
11:     $T \leftarrow T(m, n, \epsilon)$ 
12:     $t \leftarrow 0$ 
13: return  $G$ 

```
